JMEPEG (1996) 5:323-327

Development of High-Temperature Hot-Rolling Process for Grain-Oriented Silicon Steel

M. Muraki, Y. Ozaki, T. Obara, and T. Kan

A numerical study was conducted to analyze the dissolution process of manganese sulfide, and the advantages of very-high-temperature and short-time slab reheating prior to hot rolling were demonstrated. Inhibitor dissolution was greatly accelerated at elevated temperatures. High-temperature and short-time slab reheating also facilitated structure refinement by static recrystallization with appropriate rolling schedules and reduced initial grain sizes. This recrystallization also served to improve product surface quality. Another advantage of the high-temperature hot-rolling process is increased flexibility for controlling inhibitor precipitation during hot rolling.

Keywords
inhibitor, silicon steel, solution treatment, static recrystallization

1. Introduction

UNIFORM TEXTURE and finely precipitated inhibitors are important factors for achieving the uniform, stable magnetic and mechanical properties required of grain-oriented silicon steel sheet (Ref 1, 2). In order to obtain finely dispersed inhibitors, they must be fully dissolved prior to the hot-rolling process by heat treatments above the dissolution temperature, since inhibitors that precipitate upon solidification are coarse and inhomogeneously dispersed.

The introduction of a very-high-temperature slab heating process can be expected to reduce the time needed for inhibitor dissolution. This paper presents results of a numerical analysis of the dissolution of manganese sulfide at high temperatures and an investigation of the effect of temperature.

In addition, static recrystallization in 3% Si steel has recently been found to take place only after high-temperature slab heating with appropriate hot-rolling conditions (Ref 3). The effect of this recrystallization on texture refinement is also discussed.

The high-temperature hot-rolling process also allows increased flexibility in controlling inhibitor precipitation during hot rolling of grain-oriented silicon steel (Ref 4). The practical benefits achieved with this process are briefly discussed.

2. Analysis of the Dissolution Process

The dissolution process was investigated for a spherical MnS particle in 3% Si steel with a spherical cell of finite size (Fig. 1). This is the most common compound used as an inhibitor. Manganese diffusion was considered as the rate-controlling step, as sulfur diffuses much faster than manganese in α-iron (Ref 5, 6). The effects of the decomposition reaction rate of MnS, interfacial energy, and system anisotropy were neglected in the analysis.

M. Muraki, Y. Ozaki, T. Obara, and **T. Kan,** Iron and Steel Research Laboratories, Kawasaki Steel Corporation, Kurashiki, Okayama, Japan.

The solubility product of MnS in 3% Si steel was evaluated by Eq 1 (Ref 7), and the diffusivity of manganese in δ-iron expressed by Eq 2 (Ref 6) was applied to the finite-difference computation:

$$\log (\mathrm{Mn} \cdot \mathrm{S}) = \frac{-10\,590}{T + 4.092} \quad \text{(Eq 1)}$$

$$D_{\mathrm{Mn}} = 0.756 \exp\left(\frac{-224.5}{RT}\right) \quad \text{(Eq 2)}$$

where Mn and S are the concentration (mass%), T is absolute temperature, D_{Mn} is the volumetric diffusion coefficient of manganese (cm^2/s), and R is the gas constant (kJ/K · mol).

Since radial flux is the only diffusional flux that needs to be considered in a polar coordinate system, the analysis can be simplified by applying one-dimensional Eq 3:

$$\frac{\partial C}{\partial t} = D\left(\frac{\partial^2 C}{\partial r^2} + \frac{2}{r}\frac{\partial C}{\partial r}\right) \quad \text{(Eq 3)}$$

where C is the concentration of manganese, t is time (s), D is the diffusivity of manganese as a function of temperature, and r is the radius.

The average concentrations of manganese and sulfur in the system were taken as 0.08 and 0.02 mass%, respectively. The initial radius of the MnS precipitate was set at 5 μm from microscopic observation of the actual materials. A spherical cell of 70 μm radius, which was divided into 280 concentric shells, was introduced as the diffusion field. As a result of concentration of solutes to the MnS precipitate, 0.0570 mass% Mn and 0.00655 mass% S remain in the matrix (5 μm < r < 70 μm) around the precipitate (63.1 mass% Mn and 36.9 mass% S at r < 5 μm), situated at the center of the field (Fig. 1, left). This would be a stable state when silicon steel of the given composition was held at 1400 K for a long time, as judged from the solubility product (Eq 1). No diffusional flux was allowed at the outermost cell wall as a boundary condition.

3. Results and Discussion

3.1 *Dissolution Kinetics of Manganese Sulfide*

The computed changes in the manganese concentration profile in the matrix during the dissolution process are plotted in Fig. 2 (1573 K) and Fig. 3 (1673 K). In the initial stage of dissolution, the manganese concentration around the precipitate rapidly increases due to the manganese released by the decomposition of MnS, and the size of the precipitate starts to decrease. Eventually, the precipitate is thoroughly dissolved ($r/r_0 = 0$), leaving an almost uniform concentration of manganese (~0.08 mass%) in the matrix.

The advantage of high-temperature heating is increased driving force for the manganese diffusion, which results from increased solubility product of MnS (note the difference in concentration at the interface between the precipitate and matrix in Fig. 2 and 3, for example, at $r/r_0 = 0.6$, which is marked with a circle), as well as an increased diffusion coefficient of manganese.

The change in size of the MnS precipitate during the dissolution treatment is shown in Fig. 4. Manganese sulfide is dissolved relatively quickly in the initial stage, and the rate slows as the concentration of manganese around the precipitate increases (Fig. 2 and 3), regardless of temperature. As the radius approaches zero, the rate of dissolution again increases until the dissolution process is completed. Figure 4 is converted into a log scale at Fig. 5. A much shorter time is needed to dissolve MnS at the higher temperatures; for example, only 124 s (2 min) is necessary for complete dissolution at 1723 K (1450 °C). This effect of temperature would be more important in the dissolution process of MnSe in industry, since the required time for MnSe is longer than that for MnS owing to the slow diffusion of selenium.

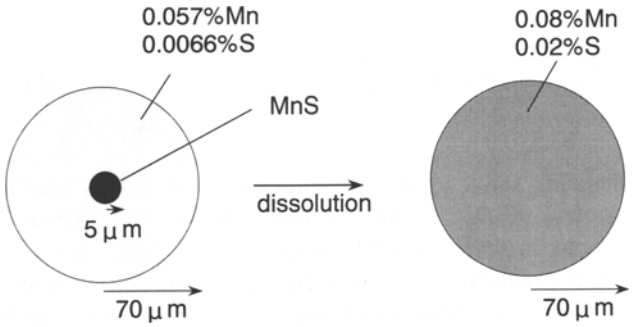

Fig. 1 Schematic representation of the calculated dissolution process

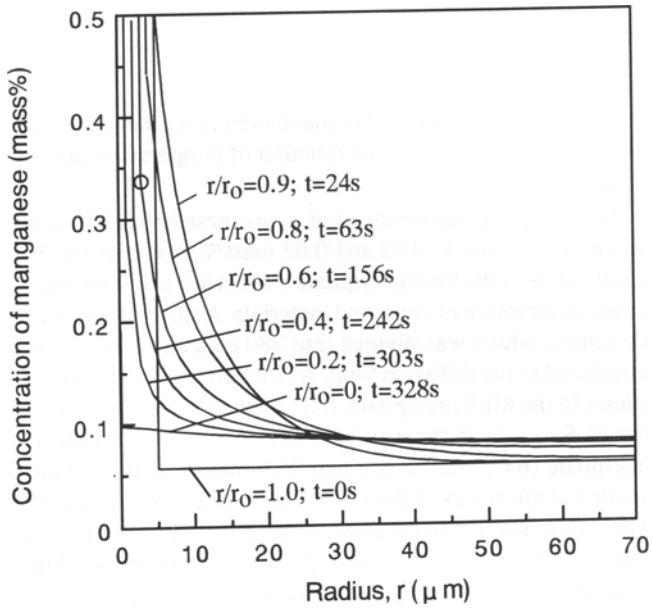

Fig. 3 Changes in the concentration profile at 1673 K

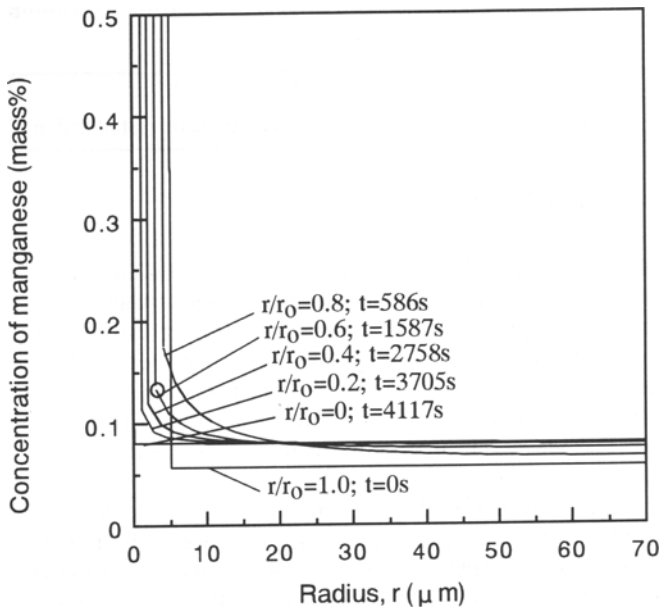

Fig. 2 Changes in the concentration profile at 1573 K

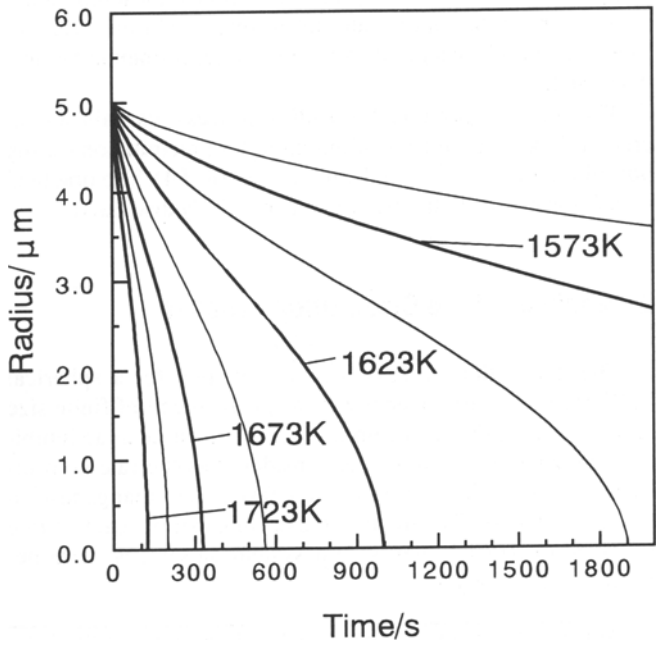

Fig. 4 Change in size of the MnS precipitate during dissolution at various temperatures

The reciprocal of the dissolution time together with D_{Mn} is plotted against $1/T$ in Fig. 6. Compared with the data at 1573 K (1300 °C), the diffusivity of manganese is increased by a factor of four at 1723 K (1450 °C), whereas the dissolution rate increases more than an order of magnitude. This difference is an effect of the increased driving force for manganese diffusion (Fig. 2 and 3), which resulted from the increased solubility product of MnS at high temperatures.

3.2 *Textural Refinement by Recrystallization*

As previously stated, silicon steel slabs are subjected to prolonged heat treatment at high temperature before hot rolling, which results in coarsened grains as large as several centimeters in size. Since some of these grains, such as the (100)[011] oriented grains, often fail to recrystallize even after cold rolling an annealing (Ref 8, 9), control of the grain size before hot rolling and of recrystallization during the hot-rolling process is important to reduce undesirable nonuniformity of texture.

Grain-growth coefficients defined after parabolic law as Eq 4 are plotted in Fig. 7 together with the relative dissolution rate of an MnS particle with an initial radius of 5 μm.

$$r^2 - r_0^2 = G \times t \qquad \text{(Eq 4)}$$

where r is the radius of the grain (cm), r_0 is the initial grain radius (cm), G is the grain-growth coefficient (cm^2/s), and t is time (s).

It is concluded from Fig. 7 that inhibitor dissolution is quickly attained compared with grain coarsening at high temperatures, even though slab grain coarsening is also accelerated with increasing temperature. The best condition for the heat treatment, therefore, would be high-temperature and short-time heating to satisfy fine slab grains and complete dissolution of inhibitor at the same time.

For the purpose of controlling recrystallization during hot rolling, Harase et al. (Ref 10) and several other researchers (Ref 11, 12) have investigated the effect of the second phase and reported that the addition of carbon and the resulting coexistence of a γ phase in silicon steel promote dynamic recrystallization during hot rolling. This effect, however, was limited to temperatures of only around 1300 K (Ref 3). Since this process cannot fully recrystallize the huge grains mentioned above at all temperatures, the undesirable nonuniformity of texture was not completely overcome.

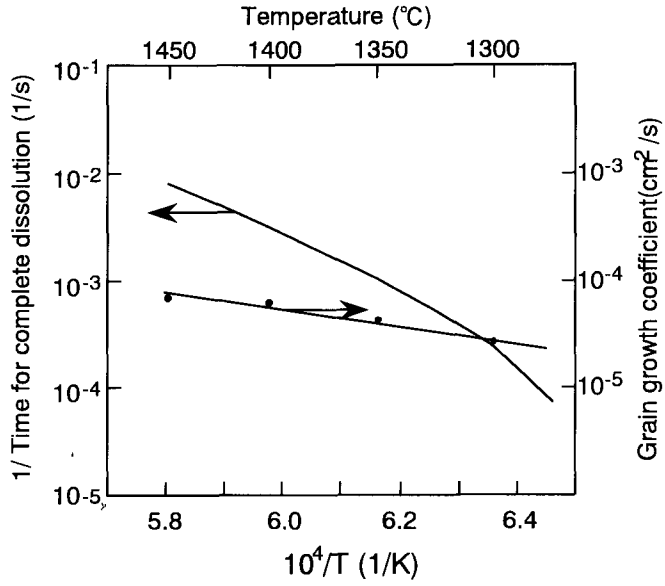

Fig. 6 Dissolution rate of a MnS particle and diffusion coefficient of manganese as a function of temperature

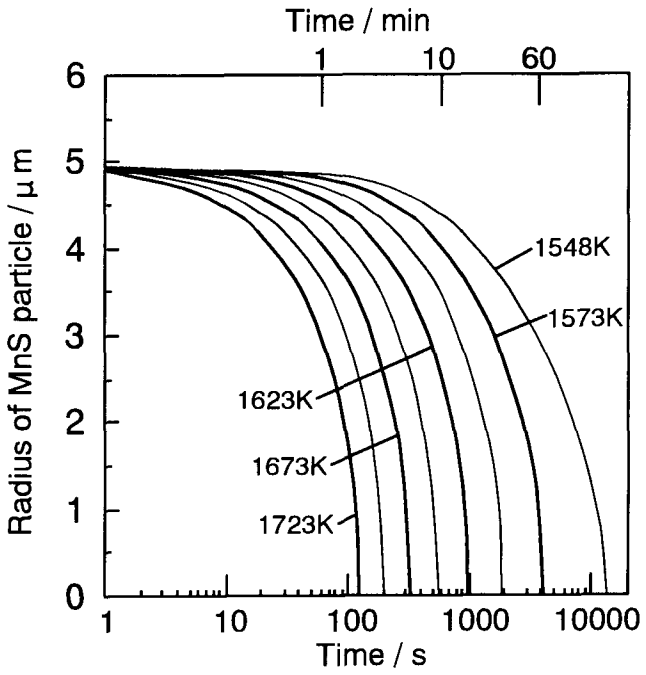

Fig. 5 Effect of slab reheating temperature on the dissolution rate of MnS in 3%-silicon steel (initial radius= 5 μm)

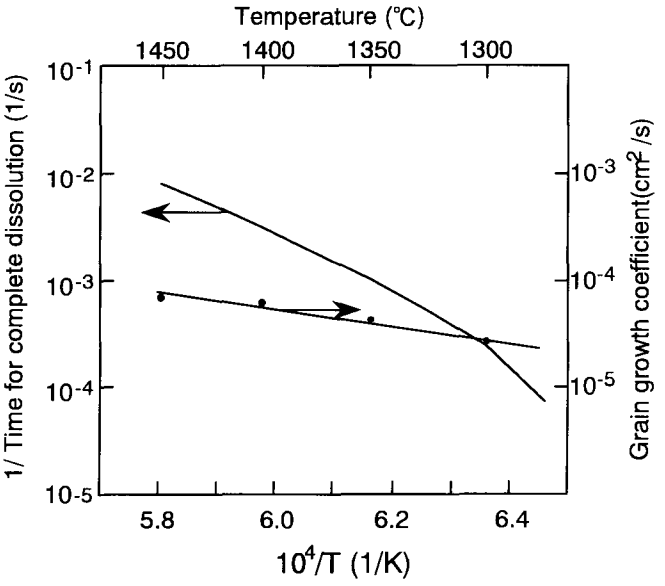

Fig. 7 Competition between inhibitor precipitation and slab grain growth

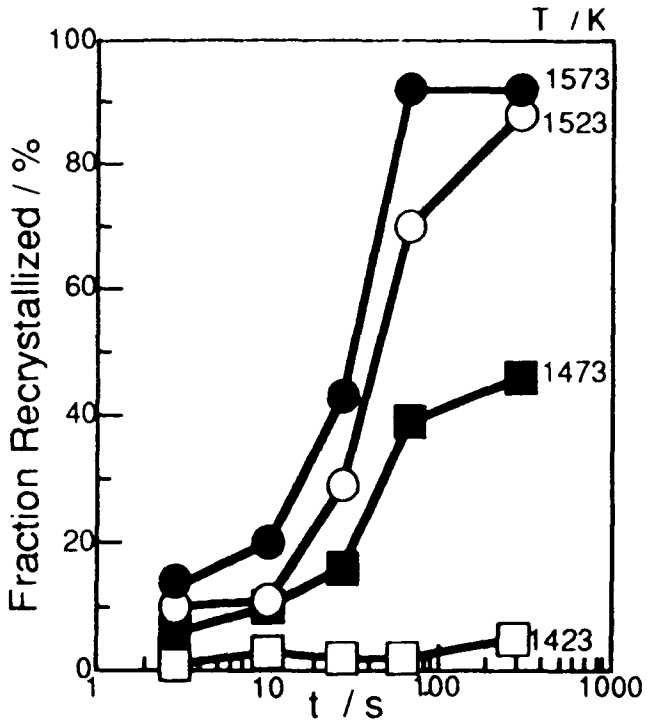

Fig. 8 Effect of holding time and temperature on the recrystallized fraction of 3% silicon steel

At higher temperatures, it has generally been accepted that recovery would dominate the restoration process in the body-centered cubic phase of silicon steel, and little attention has been paid to the recrystallization behavior above 1473 K. Manabe and several of the present authors (Ref 3, 13, 14) have previously reported that α single-phase silicon steel may statically recrystallize at a temperature between 1473 and 1673 K under suitable conditions.

The fraction recrystallized by this static recrystallization is shown in Fig. 8 as a function of the holding time after deformation. The combination of high temperature and high reduction rate with an appropriate holding time after deformation enabled complete recrystallization to be attained in the production process for 3% Si steel. By attaining recrystallization on the surface of the slab in the early stage of the hot-rolling process, improved surface quality of the product also resulted.

3.3 *Inhibitor Precipitation Control*

One of the main purposes of the hot-rolling stage for producing grain-oriented silicon steel is to achieve finely precipitated inhibitors. It is known that deformation induces inhibitor precipitation and that finely dispersed inhibitors can be obtained by deformation at a relatively low temperature, whereas coarse precipitates tend to evolve by deformation in an intermediate temperature range (Fig. 9). Deformation by hot rolling should thus be avoided during this unfavorable intermediate temperature range. The high-temperature slab heating process allows flexibility to avoid deformation at this unfavorable temperature range in the hot-rolling operation.

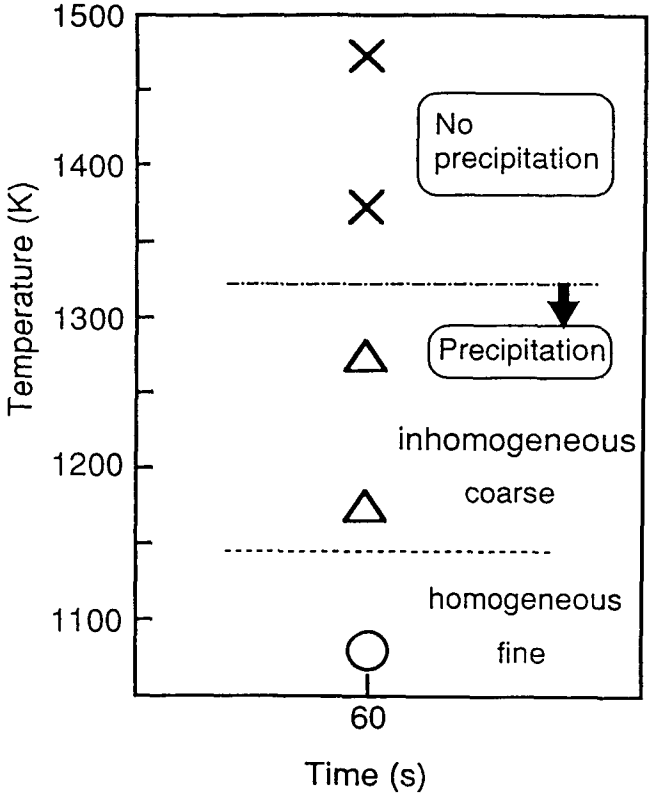

Fig. 9 Schematic drawing of the effect of deformation temperature on the dispersion of MnS

4. Summary

The introduction of a high-temperature slab heating process for grain-oriented silicon steel markedly reduced the time for inhibitor dissolution. High-temperature and short-time slab heating also enabled textural refinement by reduced size of initial grains and by static recrystallization in the α-phase region during hot rolling, which improved product surface quality at the same time. High-temperature slab heating also increased flexibility in the inhibitor precipitation during hot rolling and enabled uniform and finely dispersed inhibitor precipitation to be obtained throughout the slab length, width, and thickness.

References

1. C.G. Dunn, *Acta Metall.*, Vol 1, 1953, p 163
2. J.E. May and D. Turnbull, *Trans. Met. Soc. AIME*, Vol 212, 1958, p 769
3. M. Manabe, T. Obara, and T. Kan, *Mater. Sci. Forum*, Vol 113-115, 1993, p 491
4. T. Obara, H. Takeuchi, T. Takamiya, and T. Kan, *JMEPEG*, Vol 2, 1993, p 205
5. G. Seibel, *Mem. Sci. Rev. Metall.*, Vol 61, 1964, p 413
6. J.S. Kirkaldy, P.N. Smith, and R.C. Sharma, *Metall. Trans.*, Vol 4, 1973, p 624
7. H.A. Wriedt and Hsun Hu, *Metall. Trans. A*, Vol 7A, 1976, p 711
8. W.R. Hibbard, Jr. and W.R. Tully, *Trans. Met. Soc. AIME*, Vol 221, 1961, p 336

9. H. Hu, in *Recovery and Recrystallization of Metals,* L. Himmel, Ed., John Wiley & Sons, 1963, p 311
10. J. Harase, K. Takashima, Y. Matsumura, T. Haratani, T. Hayami, and H. Matsumoto, *Tetsu-to-Hagané (J. Iron Steel Inst. Jpn.),* Vol 67, 1981, S 1200 (in Japanese)
11. Y. Iida, H. Shimizu, Y. Ito, and H. Shimanaka, *Tetsu-to-Hagané (J. Iron Steel Inst. Jpn.),* Vol 67, 1981, S 1217 (in Japanese)
12. H.-K. Moon, *J. Korean Inst. Met.,* Vol 22, 1984, p 1176
13. M. Muraki, T. Obara, M. Satoh, and T. Kan, JMEPEG, Vol 4 No. 4, 1995 p 413
14. M. Muraki, Y. Ozaki, M. Satoh, T. Obara, and T. Kan, presented at Int. Conf. Grain Growth, Kitakyushu, Japan, 1995